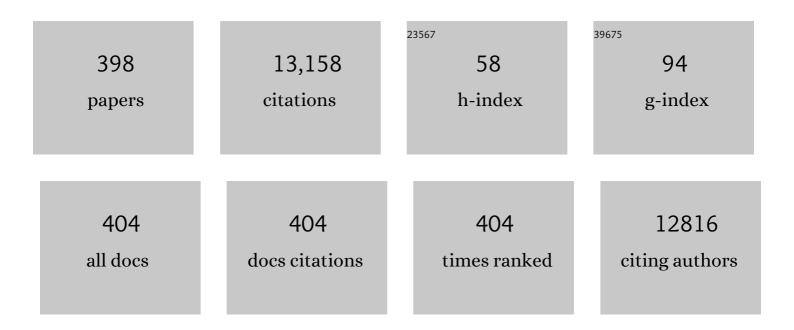
## Ashok Kumar

List of Publications by Year in descending order

Source: https://exaly.com/author-pdf/351910/publications.pdf Version: 2024-02-01



#	Article	IF	CITATIONS
1	Nuclear factor-?B: its role in health and disease. Journal of Molecular Medicine, 2004, 82, 434-48.	3.9	834
2	Nuclear factor-kappa B signaling in skeletal muscle atrophy. Journal of Molecular Medicine, 2008, 86, 1113-1126.	3.9	338
3	Sanguinarine (Pseudochelerythrine) Is a Potent Inhibitor of NF-κB Activation, IκBα Phosphorylation, and Degradation. Journal of Biological Chemistry, 1997, 272, 30129-30134.	3.4	257
4	Mechanical stress activates the nuclear factorâ€kappaB pathway in skeletal muscle fibers: a possible role in Duchenne muscular dystrophy. FASEB Journal, 2003, 17, 386-396.	0.5	244
5	Curcumin (Diferuloylmethane) Inhibition of Tumor Necrosis Factor (TNF)-Mediated Adhesion of Monocytes to Endothelial Cells by Suppression of Cell Surface Expression of Adhesion Molecules and of Nuclear Factor-κB Activation. Biochemical Pharmacology, 1998, 55, 775-783.	4.4	234
6	Gamma ray shielding properties of PbO-Li 2 O-B 2 O 3 glasses. Radiation Physics and Chemistry, 2017, 136, 50-53.	2.8	206
7	The TWEAK–Fn14 system is a critical regulator of denervation-induced skeletal muscle atrophy in mice. Journal of Cell Biology, 2010, 188, 833-849.	5.2	205
8	TNFâ€related weak inducer of apoptosis (TWEAK) is a potent skeletal muscleâ€wasting cytokine. FASEB Journal, 2007, 21, 1857-1869.	0.5	204
9	Targeted ablation of TRAF6 inhibits skeletal muscle wasting in mice. Journal of Cell Biology, 2010, 191, 1395-1411.	5.2	192
10	Barium–borate–flyash glasses: As radiation shielding materials. Nuclear Instruments & Methods in Physics Research B, 2008, 266, 140-146.	1.4	185
11	Signaling Mechanisms in Mammalian Myoblast Fusion. Science Signaling, 2013, 6, re2.	3.6	174
12	Emodin (3-methyl-1,6,8-trihydroxyanthraquinone) inhibits TNF-induced NF-κB activation, lκB degradation, and expression of cell surface adhesion proteins in human vascular endothelial cells. Oncogene, 1998, 17, 913-918.	5.9	160
13	Loss of dystrophin causes aberrant mechanotransduction in skeletal muscle fibers. FASEB Journal, 2004, 18, 102-113.	0.5	141
14	Matrix metalloproteinase-9 inhibition ameliorates pathogenesis and improves skeletal muscle regeneration in muscular dystrophy. Human Molecular Genetics, 2009, 18, 2584-2598.	2.9	141
15	Comparative study of gamma ray shielding competence of WO 3 -TeO 2 -PbO glass system to different glasses and concretes. Materials Chemistry and Physics, 2018, 213, 508-517.	4.0	140
16	Tumor Necrosis Factor-like Weak Inducer of Apoptosis Inhibits Skeletal Myogenesis through Sustained Activation of Nuclear Factor-l <sup>®</sup> B and Degradation of MyoD Protein. Journal of Biological Chemistry, 2006, 281, 10327-10336.	3.4	139
17	Emerging roles of ER stress and unfolded protein response pathways in skeletal muscle health and disease. Journal of Cellular Physiology, 2018, 233, 67-78.	4.1	135
18	The E3 Ubiquitin Ligase TRAF6 Intercedes in Starvation-Induced Skeletal Muscle Atrophy through Multiple Mechanisms. Molecular and Cellular Biology, 2012, 32, 1248-1259.	2.3	126

Ashok Kumar

#	Article	IF	CITATIONS
19	Wasting mechanisms in muscular dystrophy. International Journal of Biochemistry and Cell Biology, 2013, 45, 2266-2279.	2.8	115
20	Oxygen-Releasing Antioxidant Cryogel Scaffolds with Sustained Oxygen Delivery for Tissue Engineering Applications. ACS Applied Materials & Interfaces, 2018, 10, 18458-18469.	8.0	112
21	Dlk1 Is Necessary for Proper Skeletal Muscle Development and Regeneration. PLoS ONE, 2010, 5, e15055.	2.5	108
22	Cyclic mechanical strain inhibits skeletal myogenesis through activation of focal adhesion kinase, Racâ€1 GTPase, and NFâ€kB transcription factor. FASEB Journal, 2004, 18, 1524-1535.	0.5	105
23	Tumor Necrosis Factor-related Weak Inducer of Apoptosis Augments Matrix Metalloproteinase 9 (MMP-9) Production in Skeletal Muscle through the Activation of Nuclear Factor-ήB-inducing Kinase and p38 Mitogen-activated Protein Kinase. Journal of Biological Chemistry, 2009, 284, 4439-4450.	3.4	105
24	Physical, structural, optical and gamma ray shielding behavior of (20+x) PbO – 10 BaO – 10 Na2O – 10 MgO – (50-x) B2O3 glasses. Physica B: Condensed Matter, 2019, 552, 110-118.	2.7	102
25	Evaluation of gamma-ray and neutron shielding features of heavy metals doped Bi2O3-BaO-Na2O-MgO-B2O3 glass systems. Progress in Nuclear Energy, 2020, 118, 103118.	2.9	102
26	Mechanical and gamma-ray shielding properties of TeO2-ZnO-NiO glasses. Materials Chemistry and Physics, 2018, 212, 12-20.	4.0	100
27	<scp>ER</scp> stress in skeletal muscle remodeling and myopathies. FEBS Journal, 2019, 286, 379-398.	4.7	96
28	Experimental studies and Monte Carlo simulations on gamma ray shielding competence of (30+x)PbO 10WO3 10Na2Oâ€`â^'â€`10MgO – (40-x)B2O3 glasses. Progress in Nuclear Energy, 2020, 119, 103047.	2.9	93
29	Regulation of phosphatidylinositol 3-kinase (PI3K)/Akt and nuclear factor-kappa B signaling pathways in dystrophin-deficient skeletal muscle in response to mechanical stretch. Journal of Cellular Physiology, 2006, 208, 575-585.	4.1	92
30	Nano-Hydroxyapatite Bone Substitute Functionalized with Bone Active Molecules for Enhanced Cranial Bone Regeneration. ACS Applied Materials & Interfaces, 2017, 9, 6816-6828.	8.0	91
31	A Four-Switch Single-Stage Single-Phase Buck–Boost Inverter. IEEE Transactions on Power Electronics, 2017, 32, 5282-5292.	7.9	90
32	Mechanical stretch activates nuclear factorâ€kappaB, activator proteinâ€1, and mitogenâ€activated protein kinases in lung parenchyma: implications in asthma. FASEB Journal, 2003, 17, 1800-1811.	0.5	89
33	Zn Doped α-Fe2O3: An Efficient Material for UV Driven Photocatalysis and Electrical Conductivity. Crystals, 2020, 10, 273.	2.2	86
34	TWEAK and TRAF6 regulate skeletal muscle atrophy. Current Opinion in Clinical Nutrition and Metabolic Care, 2012, 15, 233-239.	2.5	85
35	Structural and magnetic studies of the nickel doped CoFe2O4 ferrite nanoparticles synthesized by the chemical co-precipitation method. Journal of Magnetism and Magnetic Materials, 2015, 394, 379-384.	2.3	85
36	Distinct Signaling Pathways Are Activated in Response to Mechanical Stress Applied Axially and Transversely to Skeletal Muscle Fibers. Journal of Biological Chemistry, 2002, 277, 46493-46503.	3.4	84

#	Article	IF	CITATIONS
37	Dextran based amphiphilic nano-hybrid hydrogel system incorporated with curcumin and cerium oxide nanoparticles for wound healing. Colloids and Surfaces B: Biointerfaces, 2020, 195, 111263.	5.0	84
38	The role of PbO/Bi2O3 insertion on the shielding characteristics of novel borate glasses. Ceramics International, 2020, 46, 23357-23368.	4.8	83
39	Fibroblast Growth Factor Inducible 14 (Fn14) Is Required for the Expression of Myogenic Regulatory Factors and Differentiation of Myoblasts into Myotubes. Journal of Biological Chemistry, 2007, 282, 15000-15010.	3.4	76
40	Tumor Necrosis Factor-α Regulates Distinct Molecular Pathways and Gene Networks in Cultured Skeletal Muscle Cells. PLoS ONE, 2010, 5, e13262.	2.5	76
41	Energy and chemical composition dependence of mass attenuation coefficients of building materials. Annals of Nuclear Energy, 2004, 31, 1199-1205.	1.8	75
42	CCAAT/Enhancer-binding Protein and Activator Protein-1 Transcription Factors Regulate the Expression of Interleukin-8 through the Mitogen-activated Protein Kinase Pathways in Response to Mechanical Stretch of Human Airway Smooth Muscle Cells. Journal of Biological Chemistry, 2003, 278, 18868-18876.	3.4	74
43	Genomic Profiling of Messenger RNAs and MicroRNAs Reveals Potential Mechanisms of TWEAK-Induced Skeletal Muscle Wasting in Mice. PLoS ONE, 2010, 5, e8760.	2.5	73
44	TWEAK causes myotube atrophy through coordinated activation of ubiquitinâ€proteasome system, autophagy, and caspases. Journal of Cellular Physiology, 2012, 227, 1042-1051.	4.1	72
45	Prevention of DoS Attacks in VANET. Wireless Personal Communications, 2013, 73, 95-126.	2.7	72
46	Matrix Metalloproteinase Inhibitor Batimastat Alleviates Pathology and Improves Skeletal Muscle Function in Dystrophin-Deficient mdx Mice. American Journal of Pathology, 2010, 177, 248-260.	3.8	71
47	TRAF6 coordinates the activation of autophagy and ubiquitin-proteasome systems in atrophying skeletal muscle. Autophagy, 2011, 7, 555-556.	9.1	70
48	Aligned Chitosan-Gelatin Cryogel-Filled Polyurethane Nerve Guidance Channel for Neural Tissue Engineering: Fabrication, Characterization, and In Vitro Evaluation. Biomacromolecules, 2019, 20, 662-673.	5.4	69
49	B2O3–Bi2O3–TeO2–BaO and TeO2–Bi2O3–BaO glass systems: a comparative assessment of gamma- and fast and thermal neutron attenuation aspects. Applied Physics A: Materials Science and Processing, 2020, 126, 1.	-ray 2.3	69
50	Engineering Bioinspired Antioxidant Materials Promoting Cardiomyocyte Functionality and Maturation for Tissue Engineering Application. ACS Applied Materials & Interfaces, 2018, 10, 3260-3273.	8.0	68
51	Ripple-Free Input Current High Voltage Gain DC–DC Converters With Coupled Inductors. IEEE Transactions on Power Electronics, 2019, 34, 3418-3428.	7.9	67
52	Physical, structural, optical and thermoluminescence behavior of Dy2O3 doped sodium magnesium borosilicate glasses. Results in Physics, 2019, 12, 827-839.	4.1	67
53	SnO-reinforced silicate glasses and utilization in gamma-radiation-shielding applications. Emerging Materials Research, 2020, 9, 1000-1008.	0.7	67
54	Matrix Metalloproteinase-9 Inhibition Improves Proliferation and Engraftment of Myogenic Cells in Dystrophic Muscle of mdx Mice. PLoS ONE, 2013, 8, e72121.	2.5	65

#	Article	IF	CITATIONS
55	Elevated levels of active matrix metalloproteinase-9 cause hypertrophy in skeletal muscle of normal and dystrophin-deficient mdx mice. Human Molecular Genetics, 2011, 20, 4345-4359.	2.9	63
56	The PERK arm of the unfolded protein response regulates satellite cell-mediated skeletal muscle regeneration. ELife, 2017, 6, .	6.0	63
57	Binary B2O3–Bi2O3 glasses: scrutinization of directly and indirectly ionizing radiations shielding abilities. Journal of Materials Research and Technology, 2020, 9, 14549-14567.	5.8	63
58	TNF-Like Weak Inducer of Apoptosis (TWEAK) Activates Proinflammatory Signaling Pathways and Gene Expression through the Activation of TGF-β-Activated Kinase 1. Journal of Immunology, 2009, 182, 2439-2448.	0.8	62
59	Role of nonoperative treatment in managing degenerative tears of the medial meniscus posterior root. Journal of Orthopaedics and Traumatology, 2013, 14, 193-199.	2.3	62
60	Biomimetic Photocurable Three-Dimensional Printed Nerve Guidance Channels with Aligned Cryomatrix Lumen for Peripheral Nerve Regeneration. ACS Applied Materials & Interfaces, 2018, 10, 43327-43342.	8.0	62
61	Isolation, Culturing, and Differentiation of Primary Myoblasts from Skeletal Muscle of Adult Mice. Bio-protocol, 2017, 7, .	0.4	60
62	Physiological Biomimetic Culture System for Pig and Human Heart Slices. Circulation Research, 2019, 125, 628-642.	4.5	60
63	Regulatory circuitry of TWEAKâ€Fn14 system and PGCâ€1α in skeletal muscle atrophy program. FASEB Journal, 2014, 28, 1398-1411.	0.5	59
64	Experimental and Theoretical Study of Radiation Shielding Features of CaO-K2O-Na2O-P2O5 Glass Systems. Materials, 2021, 14, 3772.	2.9	59
65	Optical, mechanical properties of TeO2-CdO-PbO-B2O3 glass systems and radiation shielding investigation using EPICS2017 library. Optik, 2021, 242, 167342.	2.9	58
66	Osteopontin-Stimulated Expression of Matrix Metalloproteinase-9 Causes Cardiomyopathy in the mdx Model of Duchenne Muscular Dystrophy. Journal of Immunology, 2011, 187, 2723-2731.	0.8	57
67	Exploration of gamma radiation shielding features for titanate bismuth borotellurite glasses using relevant software program and Monte Carlo simulation code. Journal of Non-Crystalline Solids, 2018, 481, 65-73.	3.1	57
68	TRAF6 regulates satellite stem cell self-renewal and function during regenerative myogenesis. Journal of Clinical Investigation, 2015, 126, 151-168.	8.2	57
69	TAK1 modulates satellite stem cell homeostasis and skeletal muscle repair. Nature Communications, 2015, 6, 10123.	12.8	56
70	A novel long non-coding RNA Myolinc regulates myogenesis through TDP-43 and Filip1. Journal of Molecular Cell Biology, 2018, 10, 102-117.	3.3	56
71	A novel method of utilization of hot dip galvanizing slag using the heat waste from itself for protection from radiation. Journal of Hazardous Materials, 2018, 344, 602-614.	12.4	55
72	Ferrite application as an electrochemical sensor: A review. Materials Characterization, 2021, 178, 111269.	4.4	54

Ashok Kumar

#	Article	IF	CITATIONS
73	Human immunodeficiency virus-1-tat induces matrix metalloproteinase-9 in monocytes through protein tyrosine phosphatase-mediated activation of nuclear transcription factor NF-κB. FEBS Letters, 1999, 462, 140-144.	2.8	53
74	Tumor Necrosis Factor-α Augments Matrix Metalloproteinase-9 Production in Skeletal Muscle Cells through the Activation of Transforming Growth Factor-β-activated Kinase 1 (TAK1)-dependent Signaling Pathway. Journal of Biological Chemistry, 2007, 282, 35113-35124.	3.4	53
75	Genetic Ablation of TWEAK Augments Regeneration and Post-Injury Growth of Skeletal Muscle in Mice. American Journal of Pathology, 2010, 177, 1732-1742.	3.8	53
76	TWEAK/Fn14 Signaling Axis Mediates Skeletal Muscle Atrophy and Metabolic Dysfunction. Frontiers in Immunology, 2014, 5, 18.	4.8	53
77	Noncoding RNAs in the regulation of skeletal muscle biology in health and disease. Journal of Molecular Medicine, 2016, 94, 853-866.	3.9	53
78	Decellularized Liver Matrix-Modified Cryogel Scaffolds as Potential Hepatocyte Carriers in Bioartificial Liver Support Systems and Implantable Liver Constructs. ACS Applied Materials & Interfaces, 2018, 10, 114-126.	8.0	53
79	Synthesis of Yeast-Immobilized and Copper Nanoparticle-Dispersed Carbon Nanofiber-Based Diabetic Wound Dressing Material: Simultaneous Control of Glucose and Bacterial Infections. ACS Applied Bio Materials, 2018, 1, 246-258.	4.6	52
80	Effect of PbO on the shielding behavior of ZnO–P2O5 glass system using Monte Carlo simulation. Journal of Non-Crystalline Solids, 2018, 481, 604-607.	3.1	51
81	Differences in Osmoregulation in Brassica species. Annals of Botany, 1984, 54, 537-542.	2.9	49
82	The TWEAK-Fn14 pathway: A potent regulator of skeletal muscle biology in health and disease. Cytokine and Growth Factor Reviews, 2014, 25, 215-225.	7.2	49
83	Coronavirus disease 2019 and the pancreas. Pancreatology, 2020, 20, 1567-1575.	1.1	49
84	A novel CaO–K2O–Na2O–P2O5 glass systems for radiation shielding applications. Radiation Physics and Chemistry, 2021, 188, 109645.	2.8	48
85	Therapeutic potential of matrix metalloproteinases in Duchenne muscular dystrophy. Frontiers in Cell and Developmental Biology, 2014, 2, 11.	3.7	47
86	Optical, mechanical properties and gamma ray shielding behavior of TeO2-Bi2O3-PbO-MgO-B2O3 glasses using FLUKA simulation code. Optical Materials, 2021, 113, 110900.	3.6	47
87	MyD88 promotes myoblast fusion in a cell-autonomous manner. Nature Communications, 2017, 8, 1624.	12.8	46
88	Feasibility of telemedicine in maintaining follow-up of orthopaedic patients and their satisfaction: A preliminary study. Journal of Clinical Orthopaedics and Trauma, 2020, 11, S704-S710.	1.5	46
89	PERK regulates skeletal muscle mass and contractile function in adult mice. FASEB Journal, 2019, 33, 1946-1962.	0.5	45
90	Pregnancy-associated Plasma Protein-A Regulates Myoblast Proliferation and Differentiation through an Insulin-like Growth Factor-dependent Mechanism. Journal of Biological Chemistry, 2005, 280, 37782-37789.	3.4	42

#	Article	IF	CITATIONS
91	Evaluation of pain in bilateral total knee replacement with and without tourniquet; aÂprospective randomized control trial. Journal of Clinical Orthopaedics and Trauma, 2015, 6, 85-88.	1.5	42
92	Boro-silicate glasses co-doped Er+3/Yb+3 for optical amplifier and gamma radiation shielding applications. Physica B: Condensed Matter, 2019, 567, 37-44.	2.7	42
93	Shielding behaviour of (20 + x) Bi2O3 – 20BaO–10Na2O–10MgO–(40-x) B2O3: An experimental ar Carlo study. Chemical Physics, 2020, 529, 110571.	nd Monte 1.9	42
94	Therapeutic targeting of signaling pathways in muscular dystrophy. Journal of Molecular Medicine, 2010, 88, 155-166.	3.9	40
95	ER Stress and Unfolded Protein Response in Cancer Cachexia. Cancers, 2019, 11, 1929.	3.7	40
96	Nanohydroxyapatite Based Ceramic Carrier Promotes Bone Formation in a Femoral Neck Canal Defect in Osteoporotic Rats. Biomacromolecules, 2020, 21, 328-337.	5.4	40
97	Functional and radiological outcome after delayed fixation of femoral neck fractures in pediatric patients. Journal of Orthopaedics and Traumatology, 2009, 10, 211-216.	2.3	39
98	Li2O-K2O-B2O3-PbO glass system: Optical and gamma-ray shielding investigations. Optik, 2021, 247, 167792.	2.9	39
99	Transforming Growth Factor-β-activated Kinase 1 Is an Essential Regulator of Myogenic Differentiation. Journal of Biological Chemistry, 2010, 285, 6401-6411.	3.4	38
100	TAK1 regulates skeletal muscle mass and mitochondrial function. JCI Insight, 2018, 3, .	5.0	38
101	Implementation of stacking based ARIMA model for prediction of Covid-19 cases in India. Journal of Biomedical Informatics, 2021, 121, 103887.	4.3	38
102	The Toll-Like Receptor/MyD88/XBP1 Signaling Axis Mediates Skeletal Muscle Wasting during Cancer Cachexia. Molecular and Cellular Biology, 2019, 39, .	2.3	37
103	Adipose-Derived Stem Cells (ADSCs) Loaded Gelatin-Sericin-Laminin Cryogels for Tissue Regeneration in Diabetic Wounds. Biomacromolecules, 2020, 21, 294-304.	5.4	37
104	Proinflammatory Cytokine Tumor Necrosis Factor (TNF)-like Weak Inducer of Apoptosis (TWEAK) Suppresses Satellite Cell Self-renewal through Inversely Modulating Notch and NF-κB Signaling Pathways. Journal of Biological Chemistry, 2013, 288, 35159-35169.	3.4	36
105	Finite size effect on Sm3+ doped Mn0.5Zn0.5Sm Fe2â^'O4 (0≤â‰ੳ.5) ferrite nanoparticles. Ceramics International, 2015, 41, 8623-8629.	4.8	36
106	Investigations on magnetic and electrical properties of Zn doped Fe2O3 nanoparticles and their correlation with local electronic structures. Journal of Magnetism and Magnetic Materials, 2019, 489, 165398.	2.3	36
107	Studies on the structural, optical and radiation shielding properties of (50 – x) PbO – 10 WO3–10 Na2O – 10 MgO – (20 + x) B2O3 glasses. Journal of Non-Crystalline Solids, 2019, 513, 159-166.	3.1	36
108	Theoretical and experimental validation gamma shielding properties of B2O3–ZnO–MgO–Bi2O3 glass system. Materials Chemistry and Physics, 2020, 242, 122504.	4.0	36

#	Article	IF	CITATIONS
109	Transplantation of engineered exosomes derived from bone marrow mesenchymal stromal cells ameliorate diabetic peripheral neuropathy under electrical stimulation. Bioactive Materials, 2021, 6, 2231-2249.	15.6	36
110	COMPACT PLANAR MONOPOLE UWB ANTENNA WITH QUADRUPLE BAND-NOTCHED CHARACTERISTICS. Progress in Electromagnetics Research C, 2014, 47, 29-36.	0.9	35
111	Effect of Gd3+ ion distribution on structural and magnetic properties in nano-sized Mn–Zn ferrite particles. Ceramics International, 2015, 41, 1297-1302.	4.8	35
112	Energy storage properties of double perovskites Gd2NiMnO6 for electrochemical supercapacitor application. Solid State Sciences, 2020, 105, 106252.	3.2	34
113	Transgenic Overexpression of Pregnancy-Associated Plasma Protein-A Increases the Somatic Growth and Skeletal Muscle Mass in Mice. Endocrinology, 2007, 148, 6176-6185.	2.8	33
114	Fe( <scp>iii</scp> ) induced structural, optical, and dielectric behavior of cetyltrimethyl ammonium bromide stabilized strontium stannate nanoparticles synthesized by a facile wet chemistry route. RSC Advances, 2015, 5, 17202-17209.	3.6	33
115	Detailed Inspection of γ-ray, Fast and Thermal Neutrons Shielding Competence of Calcium Oxide or Strontium Oxide Comprising Bismuth Borate Glasses. Materials, 2021, 14, 2265.	2.9	33
116	Experimental Investigation of Radiation Shielding Competence of Bi2O3-CaO-K2O-Na2O-P2O5 Glass Systems. Materials, 2021, 14, 5061.	2.9	33
117	Structural, optical and weak magnetic properties of Co and Mn codoped TiO 2 nanoparticles. Solid State Sciences, 2017, 73, 19-26.	3.2	32
118	Frequency Domain Analysis and Optimal Design of Isolated Bidirectional Series Resonant Converter. IEEE Transactions on Industry Applications, 2018, 54, 356-366.	4.9	32
119	Dual wideband circular polarized CPW-fed strip and slots loaded compact square slot antenna for wireless and satellite applications. AEU - International Journal of Electronics and Communications, 2019, 108, 181-188.	2.9	32
120	Mixed transition and rare earth ion doped borate glass: structural, optical and thermoluminescence study. Journal of Materials Science: Materials in Electronics, 2019, 30, 677-686.	2.2	32
121	Effect of prolactin on nitric oxide and interleukin-1 production of murine peritoneal macrophages: Role of Ca2+ and protein kinase C. International Journal of Immunopharmacology, 1997, 19, 129-133.	1.1	31
122	Inhibition of mechanosensitive cation channels inhibits myogenic differentiation by suppressing the expression of myogenic regulatory factors and caspaseâ€3 activity. FASEB Journal, 2005, 19, 1986-1997.	0.5	31
123	Hydrothermal synthesis and electrochemical performance of nanostructured cobalt free La2CuMnO6. Solid State Sciences, 2019, 95, 105927.	3.2	31
124	Facile wet chemical synthesis and electrochemical behavior of La2FeCoO6 nano-crystallites. Materials Science in Semiconductor Processing, 2019, 99, 8-13.	4.0	31
125	Excitatory effects of muscarine on septohippocampal neurons: involvement of M3 receptors. Brain Research, 1998, 805, 220-233.	2.2	30
126	Reciprocal Interaction between TRAF6 and Notch Signaling Regulates Adult Myofiber Regeneration upon Injury. Molecular and Cellular Biology, 2012, 32, 4833-4845.	2.3	30

#	Article	IF	CITATIONS
127	TWEAK promotes exercise intolerance by decreasing skeletal muscle oxidative phosphorylation capacity. Skeletal Muscle, 2013, 3, 18.	4.2	30
128	DNA Methyltransferase 3a and Mitogen-activated Protein Kinase Signaling Regulate the Expression of Fibroblast Growth Factor-inducible 14 (Fn14) during Denervation-induced Skeletal Muscle Atrophy. Journal of Biological Chemistry, 2014, 289, 19985-19999.	3.4	30
129	Miniaturized wideband dual linearly and circularly polarized printed square slot antenna for multiradio wireless systems. AEU - International Journal of Electronics and Communications, 2018, 88, 44-51.	2.9	30
130	Facile wet chemical synthesis of Er3+/Yb3+ co-doped BaSnO3 nano-crystallites for dye-sensitized solar cell application. Materials Science in Semiconductor Processing, 2018, 83, 83-88.	4.0	30
131	Electrochemical behavior of oxygen-deficient double perovskite, Ba2FeCoO6-Î′, synthesized by facile wet chemical process. Ceramics International, 2019, 45, 14105-14110.	4.8	30
132	Probing of nuclear radiation attenuation and mechanical features for lithium bismuth borate glasses with improving Bi2O3 content for B2O3Â+ÂLi2O amounts. Results in Physics, 2021, 25, 104246.	4.1	30
133	Evaluation of structural and gamma ray shielding competence of Li2O-K2O-B2O3-HMO (HMO =) Tj ETQq1 1 0.78-	4314 rgBT 2.9	Overlock   30
134	Midday Drop of Leaf Water Content Related to Drought Tolerance in Snap Bean (Phaseolus vulgarisL.). Plant Production Science, 2005, 8, 465-467.	2.0	29
135	Protein–DNA array-based identification of transcription factor activities differentially regulated in skeletal muscle of normal and dystrophin-deficient mdx mice. Molecular and Cellular Biochemistry, 2008, 312, 17-24.	3.1	29
136	The TWEAK–Fn14 dyad is involved in age-associated pathological changes in skeletal muscle. Biochemical and Biophysical Research Communications, 2014, 446, 1219-1224.	2.1	29
137	Electrically conductive MEH-PPV:PCL electrospun nanofibres for electrical stimulation of rat PC12 pheochromocytoma cells. Biomaterials Science, 2018, 6, 2342-2359.	5.4	29
138	Comparative study of structural, magnetic and dielectric properties of CoFe2O4 @ BiFeO3 and BiFeO3@ CoFe2O4 core-shell nanocomposites. Journal of Magnetism and Magnetic Materials, 2019, 475, 30-37.	2.3	29
139	Distinct roles of TRAF6 at early and late stages of muscle pathology in the mdx model of Duchenne muscular dystrophy. Human Molecular Genetics, 2014, 23, 1492-1505.	2.9	28
140	Microstructure and electrochemical performance of La2ZnMnO6 nanoflakes synthesized by facile hydrothermal route. Applied Physics A: Materials Science and Processing, 2020, 126, 1.	2.3	28
141	Neuroprotective Role of Oral Vitamin D Supplementation on Consciousness and Inflammatory Biomarkers in Determining Severity Outcome in Acute Traumatic Brain Injury Patients: A Double-Blind Randomized Clinical Trial. Clinical Drug Investigation, 2020, 40, 327-334.	2.2	28
142	Experimental and theoretical analysis of radiation shielding properties of strontium-borate-tellurite glasses. Optical Materials, 2021, 121, 111589.	3.6	28
143	Effect of Tumor Growth on the Blastogenic Response of Splenocytes: A Role of Macrophage-Derived Nitric Oxide. Immunological Investigations, 1996, 25, 413-423.	2.0	27
144	TeO2–B2O3–ZnO–La2O3 glasses: γ-ray and neutron attenuation characteristics analysis by WinXCOM program, MCNP5, Geant4, and Penelope simulation codes. Ceramics International, 2020, 46, 16620-16635.	4.8	27

#	Article	IF	CITATIONS
145	In-depth survey of nuclear radiation attenuation efficacies for high density bismuth lead borate glass system. Results in Physics, 2021, 23, 104030.	4.1	27
146	TRAF3IP2 mediates TWEAK/TWEAKR-induced pro-fibrotic responses in cultured cardiac fibroblasts and the heart. Journal of Molecular and Cellular Cardiology, 2018, 121, 107-123.	1.9	26
147	Local and Sustained Delivery of Rifampicin from a Bioactive Ceramic Carrier Treats Bone Infection in Rat Tibia. ACS Infectious Diseases, 2020, 6, 2938-2949.	3.8	26
148	Illustration of distinct nuclear radiation transmission factors combined with physical and elastic characteristics of barium boro-bismuthate glasses. Results in Physics, 2021, 31, 105067.	4.1	26
149	Assessing Drought Tolerance of Snap Bean (Phaseolus Vulgaris) From Genotypic Differences In Leaf Water Relations,Shoot Growth and Photosynthetic Parameters. Plant Production Science, 2007, 10, 28-35.	2.0	25
150	An offset CPW-fed triple-band circularly polarized printed antenna for multiband wireless applications. AEU - International Journal of Electronics and Communications, 2018, 86, 133-141.	2.9	25
151	Evaluating potential of tissueâ€engineered cryogels and chondrocyte derived exosomes in articular cartilage repair. Biotechnology and Bioengineering, 2022, 119, 605-625.	3.3	25
152	Toll-like receptor signalling in regenerative myogenesis: friend and foe. Journal of Pathology, 2016, 239, 125-128.	4.5	24
153	A compact printed multistubs loaded resonator rectangular monopole antenna design for multiband wireless systems. International Journal of RF and Microwave Computer-Aided Engineering, 2017, 27, e21147.	1.2	24
154	New Switching Strategy for Single-Mode Operation of a Single-Stage Buck–Boost Inverter. IEEE Transactions on Power Electronics, 2018, 33, 5927-5936.	7.9	24
155	Amine-Functionalized Electrically Conductive Core–Sheath MEH-PPV:PCL Electrospun Nanofibers for Enhanced Cell–Biomaterial Interactions. ACS Biomaterials Science and Engineering, 2018, 4, 3327-3346.	5.2	24
156	Gamma ray shielding studies on 26.66 B <sub>2</sub> O <sub>3</sub> –16GeO <sub>2</sub> –4Bi <sub>2</sub> O <sub>3</sub> –(53.33–x) PbO–xPbF <sub>2</sub> glass system using MCNPX, Geant4 and XCOM. Materials Research Express, 2018, 5, 095203.	1.6	24
157	Evaluation of optical, and radiation shielding features of New phosphate-based glass system. Optik, 2021, 242, 167220.	2.9	24
158	Molar extinction coefficients of some commonly used solvents. Radiation Physics and Chemistry, 2006, 75, 737-740.	2.8	23
159	Chitosan-Gelatin-Polypyrrole Cryogel Matrix for Stem Cell Differentiation into Neural Lineage and Sciatic Nerve Regeneration in Peripheral Nerve Injury Model. ACS Biomaterials Science and Engineering, 2019, 5, 3007-3021.	5.2	23
160	Periosteum-Mimicking Tissue-Engineered Composite for Treating Periosteum Damage in Critical-Sized Bone Defects. Biomacromolecules, 2021, 22, 3237-3250.	5.4	23
161	Improved Bone Regeneration in Rabbit Bone Defects Using 3D Printed Composite Scaffolds Functionalized with Osteoinductive Factors. ACS Applied Materials & Interfaces, 2020, 12, 48340-48356.	8.0	23
162	Design of multiâ€polarised quadâ€band planar antenna with parasitic multistubs for multiband wireless communication. IET Microwaves, Antennas and Propagation, 2018, 12, 718-726.	1.4	22

#	Article	IF	CITATIONS
163	Thermal, electrical, and dielectric properties of reduced graphene oxide–polyaniline nanotubes hybrid nanocomposites synthesized by <i>in situ</i> reduction and varying graphene oxide concentration. Journal of Applied Polymer Science, 2018, 135, 45883.	2.6	22
164	Wet chemical synthesis and electrochemical performance of novel double perovskite Y2CuMnO6 nanocrystallites. Materials Science in Semiconductor Processing, 2020, 107, 104826.	4.0	22
165	Tailoring bismuth borate glasses by incorporating PbO/GeO2 for protection against nuclear radiation. Scientific Reports, 2021, 11, 7784.	3.3	22
166	Valence shell absolute photoabsorption oscillator strengths, constrained dipole oscillator strength distributions, and dipole properties for CH3NH2, (CH3)2NH, and (CH3)3N. Canadian Journal of Chemistry, 1994, 72, 529-546.	1.1	21
167	, Effect of cisplatin and FK565 on the activation of tumor-associated and bone marrow-derived macrophages by Dalton's lymphoma. International Journal of Immunopharmacology, 1995, 17, 1-7.	1.1	21
168	Elevated levels of TWEAK in skeletal muscle promote visceral obesity, insulin resistance, and metabolic dysfunction. FASEB Journal, 2015, 29, 988-1002.	0.5	21
169	Studies on effective atomic numbers and electron densities of nucleobases in DNA. Radiation Physics and Chemistry, 2016, 127, 48-55.	2.8	21
170	Effect of novel ZnO/Zn2SnO4 photoanode on the performance of dye sensitized solar cell. Optik, 2019, 194, 163117.	2.9	21
171	Thermoluminescence, structural and optical properties of Ce3+ doped borosilicate doped glasses. Journal of Materials Science: Materials in Electronics, 2021, 32, 18381-18396.	2.2	21
172	Current strategies in tailoring methods for engineered exosomes and future avenues in biomedical applications. Journal of Materials Chemistry B, 2021, 9, 6281-6309.	5.8	21
173	Impact of Renewable Energy Sources into Multi Area Multi-Source Load Frequency Control of Interrelated Power System. Mathematics, 2021, 9, 186.	2.2	21
174	Effect of MnO on structural, optical and thermoluminescence properties of lithium borosilicate glasses. Journal of Luminescence, 2020, 219, 116872.	3.1	20
175	Solvothermal synthesis dependent structural, morphological and electrochemical behaviour of mesoporous nanorods of Sm2NiMnO6. Ceramics International, 2020, 46, 11041-11048.	4.8	20
176	Physical, optical, structural and thermoluminescence behaviour of borosilicate glasses doped with trivalent neodymium ions. Optical Materials, 2021, 117, 111109.	3.6	20
177	Optical and gamma-ray shielding effectiveness of a newly fabricated P2O5–CaO–Na2O–K2O–PbO glass system. Progress in Nuclear Energy, 2021, 138, 103798.	2.9	20
178	Assay for redox-sensitive kinases. Methods in Enzymology, 1999, 300, 339-345.	1.0	19
179	Cetyltriammonium Bromide Assisted Synthesis of Lanthanum Containing Barium Stannate Nanoparticles for Application in Dye Sensitized Solar Cells. Physica Status Solidi (A) Applications and Materials Science, 2018, 215, 1700723.	1.8	19
180	Extensive study of newly developed highly dense transparent PbO-WO3-BaO-Na2O-B2O3 glasses for radiation shielding applications. Journal of Non-Crystalline Solids, 2019, 521, 119521.	3.1	19

#	Article	IF	CITATIONS
181	Effects of different concentration and combinations of cryoprotectants on sperm quality, functional integrity in three Indian horse breeds. Cryobiology, 2019, 86, 52-57.	0.7	19
182	Canonical NF-κB signaling regulates satellite stem cell homeostasis and function during regenerative myogenesis. Journal of Molecular Cell Biology, 2019, 11, 53-66.	3.3	19
183	Endogenous Platelet-Rich Plasma Supplements/Augments Growth Factors Delivered via Porous Collagen-Nanohydroxyapatite Bone Substitute for Enhanced Bone Formation. ACS Biomaterials Science and Engineering, 2019, 5, 56-69.	5.2	19
184	On the anisotropy of the triple-dipole dispersion energy for interactions involving linear molecules. Molecular Physics, 1996, 87, 845-858.	1.7	18
185	Dipole polarizability, sum rules, mean excitation energies, and long-range dispersion coefficients for buckminsterfullerene C60. Chemical Physics Letters, 2011, 516, 208-211.	2.6	18
186	Gamma ray shielding behavior of Li2O-doped PbO–MoO3–B2O3 glass system. Applied Physics A: Materials Science and Processing, 2019, 125, 1.	2.3	18
187	Wideband circularly polarized parasitic patches loaded coplanar waveguide-fed square slot antenna with grounded strips and slots for wireless communication systems. AEU - International Journal of Electronics and Communications, 2020, 114, 153011.	2.9	18
188	Structural and paramagnetic resonance properties correlation in lanthanum ion doped nickel ferrite nanoparticles. Journal of Magnetism and Magnetic Materials, 2020, 508, 166866.	2.3	18
189	Investigation of the optical, mechanical, and radiation shielding features for strontium-borotellurite glass system: Fabrication, characterization, and EPICS2017 computations. Optik, 2021, 243, 167468.	2.9	18
190	The physical, structural and the gamma ray shielding effectiveness of the novel Li2O-K2O–B2O3–TeO2 glasses. Results in Physics, 2021, 29, 104726.	4.1	18
191	Isolation, Culture, and Staining of Single Myofibers. Bio-protocol, 2016, 6, .	0.4	18
192	Assessment of gamma-rays and fast neutron beam attenuation features of Er2O3-doped B2O3–ZnO–Bi2O3 glasses using XCOM and simulation codes (MCNP5 and Geant4). Applied Physics A: Materials Science and Processing, 2019, 125, 1.	2.3	17
193	Comparative study of gamma-ray shielding features and some properties of different heavy metal oxide-based tellurite-rich glass systems. Radiation Physics and Chemistry, 2020, 170, 108633.	2.8	17
194	Structural, optical and thermoluminescence properties of newly developed MnKB: Er3+ glass system. Journal of Non-Crystalline Solids, 2020, 543, 120113.	3.1	17
195	Alternate pathway for standard SCR on Cu-zeolites with gas-phase ammonia. Reaction Chemistry and Engineering, 2021, 6, 1042-1052.	3.7	17
196	Data supporting exosome laden oxygen releasing antioxidant and antibacterial cryogel wound dressing OxOBand alleviate diabetic and infectious wound healing. Data in Brief, 2020, 31, 105671.	1.0	16
197	Ethylene glycol/citric acid stabilized wet chemically synthesized Y2CoNiO6, and its structural, dielectric, magnetic and electrochemical behavior. Journal of Materials Science: Materials in Electronics, 2020, 31, 6977-6987.	2.2	16
198	Understanding the role of Bi2O3 in the P2O5–CaO–Na2O–K2O glass system in terms of physical, structural and radiation shielding properties. Journal of Materials Science: Materials in Electronics, 2021, 32, 11649-11665.	2.2	16

#	Article	IF	CITATIONS
199	Exosome-Functionalized Ceramic Bone Substitute Promotes Critical-Sized Bone Defect Repair in Rats. ACS Applied Bio Materials, 2021, 4, 3716-3726.	4.6	16
200	Mechanical and Gamma Ray Absorption Behavior of PbO-WO3-Na2O-MgO-B2O3 Glasses in the Low Energy Range. Materials, 2021, 14, 3466.	2.9	16
201	Distinct roles of TRAF6 and TAK1 in the regulation of adipocyte survival, thermogenesis program, and high-fat diet-induced obesity. Oncotarget, 2017, 8, 112565-112583.	1.8	16
202	RF parameter extraction of MMIC nichrome resistors. Microwave and Optical Technology Letters, 2003, 39, 409-412.	1.4	15
203	Low grade central osteosarcoma – A diagnostic dilemma. Joint Bone Spine, 2008, 75, 613-615.	1.6	15
204	Radiation shielding parameters of BaO–Nb <sub>2</sub> O <sub>5</sub> –P <sub>2</sub> O <sub>5</sub> glass system using MCNP5 code and XCOM software. Materials Research Express, 2018, 5, 115203.	1.6	15
205	MyD88 is required for satellite cell-mediated myofiber regeneration in dystrophin-deficient mdx mice. Human Molecular Genetics, 2018, 27, 3449-3463.	2.9	15
206	Electrocatalytic Acitivity of rGO/PEDOT : PSS Nanocomposite towards Methanol Oxidation in Alkaline Media. Electroanalysis, 2018, 30, 2131-2144.	2.9	15
207	Optically transparent newly developed glass materials for gamma ray shielding applications. Journal of Non-Crystalline Solids, 2019, 521, 119490.	3.1	15
208	Surface modification of reduced graphene oxideâ€polyaniline nanotubes nanocomposites for improved supercapacitor electrodes. Polymer Composites, 2020, 41, 653-667.	4.6	15
209	Enhanced bone mineralization using hydroxyapatite-based ceramic bone substitute incorporating <i>Withania somnifera</i> extracts. Biomedical Materials (Bristol), 2020, 15, 055015.	3.3	15
210	Synthesis and biological activity of isodithiobiurets, dithiobiurets, and dithiazoles. Pharmaceutical Research, 1987, 04, 321-326.	3.5	14
211	A novel single stage, transformerless PV inverter. , 2014, , .		14
212	Cetyltrimethyl ammonium bromide stabilized lanthanum doped SrSnO3 nanoparticle photoanode for dye sensitized solar cell application. Solid State Communications, 2018, 269, 6-10.	1.9	14
213	Probing the ionic transport dynamics in ionic liquid incorporated CuBTC-Metal-Organic Framework based PVdF-HFP nanocomposite membranes. Solid State Sciences, 2020, 100, 106115.	3.2	14
214	Agar–lodine Transdermal Patches for Infected Diabetic Wounds. ACS Applied Bio Materials, 2020, 3, 7515-7530.	4.6	14
215	Optimization Methodologies and Testing on Standard Benchmark Functions of Load Frequency Control for Interconnected Multi Area Power System in Smart Grids. Mathematics, 2020, 8, 980.	2.2	14
216	Li2O–B2O3–Bi2O3 glasses: gamma-rays and neutrons attenuation study using ParShield/WinXCOM program and Geant4 and Penelope codes. Applied Physics A: Materials Science and Processing, 2020, 126, 1.	2.3	14

#	Article	IF	CITATIONS
217	A comprehensive investigation on the role of PbO in the structural and radiation shielding attribute of P2O5–CaO–Na2O–K2O–PbO glass system. Journal of Materials Science: Materials in Electronics, 2021, 32, 12371-12382.	2.2	14
218	Gamma-ray shielding, physical, and structural characteristics of TeO2–CdO–PbO–B2O3 glasses. Optical Materials, 2021, 119, 111333.	3.6	14
219	SrO-SiO2-B2O3-ZrO2 glass system: Effects of varying SrO and BaO compositions to physical and optical properties, and radiation shielding using EPDL2017 photoatomic library. Optik, 2021, 245, 167670.	2.9	14
220	Intra-articular gold induced cytokine (GOLDIC®) injection therapy in patients with osteoarthritis of knee joint: a clinical study. International Orthopaedics, 2021, 45, 497-507.	1.9	14
221	A Synthetic Peptide, L-8-K, and Its Antibody Both Inhibit the Specific Binding of Vasoactive Intestinal Peptide to Hamster Pancreatic Cancer Cells. Annals of the New York Academy of Sciences, 1988, 527, 679-681.	3.8	13
222	Effect of cisplatin administration on the proliferation and differentiation of bone marrow cells of tumourâ€bearing mice. Immunology and Cell Biology, 1995, 73, 220-225.	2.3	13
223	Effect of Dalton's lymphoma on the antigen presentation of murine peritoneal macrophages. Cancer Letters, 1995, 92, 151-157.	7.2	13
224	ACCIDENTALLY FALLING INSTRUMENTS DURING ORTHOPAEDIC SURGERY: TIME TO WAKE UP!. ANZ Journal of Surgery, 2008, 78, 794-795.	0.7	13
225	Compact printed ultra-wideband antenna with two notched stop bands for WiMAX and WLAN. International Journal of Applied Electromagnetics and Mechanics, 2015, 47, 523-531.	0.6	13
226	Structural, optical, and gamma-ray-sensing characterization of (35Ââ^'Âx) PbO–10 MgO–10Na2O–5 Fe2O3–10 BaO–(30Ââ^'Âx) B2O3 glasses. Applied Physics A: Materials Science and Processing, 2019, 125, 1	. <sup>2.3</sup>	13
227	A broadband circularly polarized monopole antenna for millimeterâ€wave short range 5G wireless communication. International Journal of RF and Microwave Computer-Aided Engineering, 2021, 31, e22518.	1.2	13
228	Elastic scattering of electrons by argon atoms. Pramana - Journal of Physics, 1978, 10, 63-73.	1.8	12
229	Effect of finite sample dimensions and total scatter acceptance angle on the gamma ray buildup factor. Annals of Nuclear Energy, 2008, 35, 2414-2416.	1.8	12
230	Investigation of structural, morphological and electrochemical properties of mesoporous La2CuCoO6 rods fabricated by facile hydrothermal route. International Journal of Minerals, Metallurgy and Materials, 2020, 27, 987-995.	4.9	12
231	Mesoporous spheres of Dy2NiMnO6 synthesized via hydrothermal route for structural, morphological, and electrochemical investigation. Ionics, 2020, 26, 5143-5153.	2.4	12
232	Influence of High Temperature on Morphological Characters, Biomass Allocation, and Yield Components in Snap Bean (Phaseolus vulgarisL.). Plant Production Science, 2006, 9, 200-205.	2.0	11
233	Kimura disease of extremity: Unusual manifestation in a long bone. Joint Bone Spine, 2008, 75, 492-494.	1.6	11
234	Compact elliptical microstrip patch antenna with slotted ground for Ku-band applications. , 2011, , .		11

#	Article	IF	CITATIONS
235	Annealing effect on the structural and dielectric properties of hematite nanoparticles. AIP Conference Proceedings, 2018, , .	0.4	11
236	Influence of Ce3+ Ion Doping on Structural and Magnetic Properties of Magnesium Nanoferrite. Journal of Superconductivity and Novel Magnetism, 2019, 32, 1465-1474.	1.8	11
237	Facile solvothermal synthesis of nano-assembled mesoporous rods of cobalt free – La2NiFeO6 for electrochemical behaviour. Materials Science and Engineering B: Solid-State Materials for Advanced Technology, 2020, 261, 114664.	3.5	11
238	TAK1 preserves skeletal muscle mass and mitochondrial function through redox homeostasis. FASEB BioAdvances, 2020, 2, 538-553.	2.4	11
239	Synthesis and Behavior of Cetyltrimethyl Ammonium Bromide Stabilized Zn1+xSnO3+x (0 ≤ â‰⊈) Nano-Crystallites. PLoS ONE, 2016, 11, e0156246.	2.5	11
240	The IRE1/XBP1 signaling axis promotes skeletal muscle regeneration through a cell non-autonomous mechanism. ELife, 2021, 10, .	6.0	11
241	Reckoning of nuclear radiation attenuation capabilities for binary GeO2-Tl2O, GeO2-Bi2O3, and ternary GeO2-Tl2O–Bi2O3 glasses utilizing pertinent theoretical and computational approaches. Optical Materials, 2020, 108, 110113.	3.6	10
242	Oxidised charcoal: an efficient support for NiFe layered double hydroxide to improve electrochemical oxygen evolution. Chemical Communications, 2020, 56, 8770-8773.	4.1	10
243	Biofabrication of gold nanoparticles with bone remodeling potential: an in vitro and in vivo assessment. Journal of Nanoparticle Research, 2020, 22, 1.	1.9	10
244	Mechanical and photon shielding aspects of PbO–BaO–WO3–Na2O–B2O3 glass systems. Applied Physics A: Materials Science and Processing, 2021, 127, 1.	2.3	10
245	Corrosion inhibition of nickel in 4% nitric acid by substituted thione compounds. Materials Chemistry and Physics, 1998, 56, 243-248.	4.0	9
246	Influence Of Temperature Shift After Flowering on Dry Matter Partitioning In Two Cultivars of Snap Bean (Phaseolus Vulgaris)That Differ In Heat Tolerance. Plant Production Science, 2007, 10, 14-19.	2.0	9
247	Do locking plates have a role in orthopaedic oncological reconstruction. Archives of Orthopaedic and Trauma Surgery, 2010, 130, 1493-1497.	2.4	9
248	A compact ultra-wideband CPW-fed printed antenna with SRR for rejecting WLAN band. , 2011, , .		9
249	Bizarre parosteal osteochondromatous proliferation (Nora's lesion) of phalanx in a child. BMJ Case Reports, 2014, 2014, bcr2013201714-bcr2013201714.	0.5	9
250	Up-Conversion in Perovskite Strontium Stannate Nanocrystal Whiskers. Transactions of the Indian Institute of Metals, 2017, 70, 573-579.	1.5	9
251	Structural, Optical, and Multiferroic Properties of Yttrium (Y3+)-Substituted BiFeO3 Nanostructures. Journal of Superconductivity and Novel Magnetism, 2020, 33, 2017-2029.	1.8	9
252	Rare-earth (Dy)-doped (GeS2)80(In2S3)20 thin film: influence of annealing temperature in argon environment on the linear and nonlinear optical parameters. Applied Physics A: Materials Science and Processing, 2021, 127, 1.	2.3	9

#	Article	IF	CITATIONS
253	Synthesis, structural investigation, mechanical calculations and photon shielding properties of CaO–K2O–Na2O–P2O5 glass system. Optical Materials, 2021, 117, 111178.	3.6	9
254	Gene Profiling Studies in Skeletal Muscle by Quantitative Real-Time Polymerase Chain Reaction Assay. Methods in Molecular Biology, 2012, 798, 311-324.	0.9	9
255	Prevalence and risk factors for nonalcoholic fatty liver disease in obese children in rural Punjab, India. Journal of Family and Community Medicine, 2020, 27, 103.	1.1	9
256	H19Xâ€encoded miRâ€322(424)/miRâ€503 regulates muscle mass by targeting translation initiation factors. Journal of Cachexia, Sarcopenia and Muscle, 2021, 12, 2174-2186.	7.3	9
257	Studies on Effective Atomic Numbers and Electron Densities in Some Commonly Used Solvents. Nuclear Science and Engineering, 2007, 155, 102-108.	1.1	8
258	An unusual presentation of a rare chest wall tumour: Giant cell tumour of bone. Joint Bone Spine, 2007, 74, 100-102.	1.6	8
259	Measurements of linear attenuation coefficients of irregular shaped samples by two media method. Nuclear Instruments & Methods in Physics Research B, 2008, 266, 1116-1121.	1.4	8
260	A SEPIC derived single stage buck-boost inverter for photovoltaic applications. , 2014, , .		8
261	Functional improvement after hip arthroscopy in cases of active paediatric hip joint tuberculosis: A retrospective comparative study vis-Ã-vis conservative management. Journal of Children's Orthopaedics, 2015, 9, 495-503.	1.1	8
262	Reconfigurable circular disc monopole UWB antenna with switchable two notched stop bands. , 2016, , .		8
263	Effects of omega-3 on matrix metalloproteinase-9, myoblast transplantation and satellite cell activation in dystrophin-deficient muscle fibers. Cell and Tissue Research, 2017, 369, 591-602.	2.9	8
264	Quality assurance and adverse event management in regenerative medicine for knee osteoarthritis: Current concepts. Journal of Clinical Orthopaedics and Trauma, 2019, 10, 53-58.	1.5	8
265	Gelatin interpenetration in poly N â€isopropylacrylamide network reduces the compressive modulus of the scaffold: A property employed to mimic hepatic matrix stiffness. Biotechnology and Bioengineering, 2020, 117, 567-579.	3.3	8
266	Structural and multiferroic properties of BiFeO3/MgLa0.025Fe1.975O4 nanocomposite synthesized by sol–gel auto combustion route. Journal of Materials Science: Materials in Electronics, 2020, 31, 2777-2788.	2.2	8
267	Fabrication of TeO2-doped strontium borate glasses possessing optimum physical, structural, optical and gamma ray shielding properties. European Physical Journal Plus, 2021, 136, 1.	2.6	8
268	Gangliosides Produced by a T Cell Lymphoma Inhibit the Production of Reactive Nitrogen Intermediates by Murine Peritoneal Macrophages Journal of Clinical Biochemistry and Nutrition, 1996, 21, 171-182.	1.4	8
269	Impact of Bi2O3 on optical properties and radiation attenuation characteristics of Bi2O3-Li2O-P2O5 glasses. Optik, 2021, 248, 168081.	2.9	8
270	The absorption coefficient spectrum of poly(methyl methacrylate) in the soft X-ray region. Journal of Polymer Science, Part B: Polymer Physics, 1992, 30, 185-195.	2.1	7

#	Article	IF	CITATIONS
271	Adaptation to Heat and Drought Stresses in Snap Bean (Phaseolus vulgaris) during the Reproductive Stage of Development. Japan Agricultural Research Quarterly, 2006, 40, 213-216.	0.4	7
272	Dual band-notched circular disc monopole UWB antenna with switchable five notched stop bands. , 2016, , .		7
273	Investigations on structural and magnetic properties of Mn doped Er 2 O 3. Solid State Sciences, 2017, 67, 8-12.	3.2	7
274	Size dependent morphology, magnetic and dielectric properties of BiFeO3 nanoparticles. MRS Advances, 2019, 4, 1659-1665.	0.9	7
275	MINIATURIZED MULTISTUBS LOADED RECTANGULAR MONOPOLE ANTENNA FOR MULTIBAND APPLICATIONS BASED ON THEORY OF CHARACTERISTICS MODES. Progress in Electromagnetics Research C, 2019, 92, 177-189.	0.9	7
276	An Offset CPW-Fed Dual-Band Circularly Polarized Printed Antenna for Multiband Wireless Applications. Lecture Notes in Electrical Engineering, 2020, , 411-418.	0.4	7
277	Response to a Fire Incident in the Operation Room: A Cautionary Tale. Disaster Medicine and Public Health Preparedness, 2020, 14, 284-288.	1.3	7
278	Letter to the editor in response to COVID-19 presenting as acute pancreatitis. Pancreatology, 2020, 20, 1021-1022.	1.1	7
279	Multidimensional dynamic healthcare personnel (HCP)-centric model from a low-income and middle-income country to support and protect COVID-19 warriors: a large prospective cohort study. BMJ Open, 2021, 11, e043837.	1.9	7
280	Physical, structural, and gamma ray shielding studies on novel (35+x) PbO-5TeO2-20Bi2O3-(20-x) MgO-20B2O3 glasses. Journal of the Australian Ceramic Society, 2021, 57, 971-981.	1.9	7
281	Spinal cord regeneration: A brief overview of the present scenario and a sneak peek into the future. Biotechnology Journal, 2021, 16, e2100167.	3.5	7
282	Impedance analysis and dielectric response of anatase TiO <sub>2</sub> nanoparticles codoped with Mn and Co ions. Materials Research Express, 2017, 4, 115035.	1.6	6
283	Nickel-induced magnetic behaviour of nano-structured α-Fe <sub>2</sub> O <sub>3</sub> , synthesised by facile wet chemical route. Philosophical Magazine, 2018, 98, 2425-2439.	1.6	6
284	Critical points for electron–Mg atom elastic scattering. Journal of Physics B: Atomic, Molecular and Optical Physics, 2018, 51, 035203.	1.5	6
285	Phase transformation in wet chemically synthesized Y2NiFeO6, and its magnetic and energy storage properties. Applied Physics A: Materials Science and Processing, 2020, 126, 1.	2.3	6
286	Structural, Dielectric, and Energy Storage Properties of Citric Acid and Ethylene Glycol Assisted Hydrothermally Synthesized Y <sub>2</sub> FeCoO <sub>6</sub> . Physica Status Solidi (A) Applications and Materials Science, 2020, 217, 2000324.	1.8	6
287	Performance Analysis of Underwater 2D OCDMA System. Lecture Notes in Electrical Engineering, 2020, , 477-484.	0.4	6
288	A Prospective Study of Novel Therapeutic Targets Interleukin 6, Tumor Necrosis Factor α, and Interferon γ as Predictive Biomarkers for the Development of Posttraumatic Epilepsy. World Neurosurgery: X, 2021, 12, 100107.	1.1	6

#	Article	IF	CITATIONS
289	Ultra-wideband truncated rectangular monopole antenna with band-notched characteristics. , 2012, , .		5
290	A high voltage gain current fed non-isolated dc-dc converter. , 2016, , .		5
291	A quad-band reconfigurable microstrip-fed circular disc monopole antenna for multiradio wireless systems. , 2016, , .		5
292	Composite bilayered scaffolds with bio-functionalized ceramics for cranial bone defects: An <i>in vivo</i> evaluation. Multifunctional Materials, 2019, 2, 014002.	3.7	5
293	A study of critical minima and spin polarization in the e±–Ba elastic scattering. European Physical Journal D, 2020, 74, 1.	1.3	5
294	Perioperative COVID-19 testing for orthopaedic patients: Current evidence. Journal of Clinical Orthopaedics and Trauma, 2020, 11, S296-S297.	1.5	5
295	Recent Advances in Biomaterialâ€Based Highâ€Throughput Platforms. Biotechnology Journal, 2021, 16, 2000288.	3.5	5
296	Tailoring Dy3+/Tb3+-doped lead telluride borate glasses for gamma-ray shielding applications. European Physical Journal Plus, 2021, 136, 1.	2.6	5
297	Gamma ray interaction studies of the PbCl2–SnCl2–P2O5 bioactive glass system for applications in nuclear medicine. Journal of the Australian Ceramic Society, 2021, 57, 635-642.	1.9	5
298	Pes Anserinus Bursitis due to Tibial Spurs in Children. Cureus, 2017, 9, e1427.	0.5	5
299	Total cross sections for positron scattering from argon atoms at intermediate energies. Physical Review A, 1986, 33, 2795-2797.	2.5	4
300	An Improved Model for GaAs MESFETs Suitable for a Wide Bias Range. IEEE Microwave and Wireless Components Letters, 2007, 17, 52-54.	3.2	4
301	Direct Repair without Augmentation of Patellar Tendon Avulsion following TKA. Case Reports in Orthopedics, 2015, 2015, 1-4.	0.3	4
302	Dipole properties of PH3, PF3, PF5, PCl3, SiCl4, GeCl4, and SnCl4. Molecular Physics, 2016, 114, 1657-1663.	1.7	4
303	A compact triple-band planar MIMO diversity antenna for WiMAX/WLAN applications. , 2017, , .		4
304	Morphology correlated efficiency of ZnO photoanode in dye sensitized solar cell. Materials Research Express, 2019, 6, 1050d3.	1.6	4
305	Elastic scattering of electrons by Sr atom: a study of critical minima and spin polarization. Journal of Physics Communications, 2019, 3, 065001.	1.2	4
306	Facile synthesis of novel ZnO/Cd0.5Zn0.5S photoanode for dye-sensitized solar cell. Materials Research Express, 2019, 6, 085029.	1.6	4

IF # ARTICLE CITATIONS 100 MeV O<sup>7+</sup> ion irradiation induced electrochemical enhancement in NiBTC metal-organic framework based composite polymer electrolytes incorporated with ionic liquid. Materials Research Express, 2019, 6, 085305. A Cascaded Buck-Flyback Structure for High Voltage Step Down Applications., 2019, , . 308 4 Studies of Various Artificial Magnetic Conductor for 5G Applications. Lecture Notes in Electrical 309 0.4 Engineering, 2020, , 523-530. rGO/PEDOT:PSS/NiMn<sub>2</sub>O<sub>4</sub> Nanohybrid: An Inexpensive Anode Catalyst for Methanol and Ethylene Glycol Electro-Oxidation. Journal of the Electrochemical Society, 2021, 168, 310 2.9 4 034510. Facile wet chemical synthesis and electrochemical performance of double perovskite- La2NiMnO6 for 311 1.8 energy storage application. Materials Today: Proceedings, 2022, 48, 587-589. Miniaturized High-Power Beam Steering Network Using Novel Nonplanar Waveguide Butler Matrix. IEEE Microwave and Wireless Components Letters, 2021, 31, 678-681. 312 3.2 4 Dielectric constant, polarizability, susceptibility and gamma ray shielding behavior of the Li2O-Li2MoO4-TiO2-P2O5 glasses. Optik, 2021, 245, 167639. 2.9 4 Effects of Sm3+ ions on the structural, optical and thermoluminescence properties of MnKB glass 314 4.0 4 system. Journal of Physics and Chemistry of Solids, 2022, 161, 110408. Regulation of Intracellular Signal Transduction Pathways by Mechanosensitive Ion Channels., 2008, 303-327. Endotoxin-induced protein phosphorylation in macrophages is modulated by tumor cells. 316 1.1 3 International Journal of Immunopharmacology, 1998, 20, 99-110. Reliable results for the Isotropic Dipole – Dipole and Triple – Dipole Dispersion Energy Coefficients for Interactions involving Formaldehyde, Acetaldehyde, Acetone, and Mono'-, Di-, and Tri 0.2 Methylamine. Journal of Computational Methods in Sciences and Engineering, 2004, 4, 307-320. A rare actinomycosis of humerus: an unusual location and a diagnostic dilemma. A case report. 318 2.4 3 Archives of Orthopaedic and Trauma Surgery, 2007, 128, 121-124. Design and analysis of CPW-fed quasi-self-complementary pentagonal antenna for ultra-wideband systems., 2014, , . Analysis and design of a current fed non-isolated buck-boost DC-DC converter., 2016, , . 320 3 Design of reconfigurable compact dual polarized antenna for multiband operation., 2017,,. A compact offset CPW-fed dual polarized stubs loaded monopole antenna for quad-band operation., 322 3 2017, , . Compact offset CPW-fed inverted L-shaped dual-band dual-polarized reconfigurable printed antenna., 2017,,. Compact Triple-Band Stubs-Loaded Rectangular Monopole Antenna for WiMAX/WLAN Applications. 324 0.4 3 Lecture Notes in Electrical Engineering, 2018, , 429-435.

#	Article	IF	CITATIONS
325	Design and Studies of Bandstop Filters Using Modified CSRR DGS for WLAN Applications. Lecture Notes in Electrical Engineering, 2020, , 467-475.	0.4	3
326	Mapping B-Cell Epitopes for Nonspecific Lipid Transfer Proteins of Legumes Consumed in India and Identification of Critical Residues Responsible for IgE Binding. Foods, 2021, 10, 1269.	4.3	3
327	Prevalence of 25-Hydroxyvitamin D Deficiency and its severity correlation with Acute Traumatic brain Injury in Indian Patients: A Perspective Observation Study. Research Journal of Pharmacy and Technology, 2021, , 3874-3878.	0.8	3
328	Effect of adding SrO, TeO2, PbO, and Bi2O3 heavy metal oxides on the optical and gamma ray shielding properties of Li2O-K2O-B2O3 glasses. Optik, 2021, 247, 167848.	2.9	3
329	Influence of Irrigation Level, Growth Stages and Cultivars on Leaf Gas Exchange Characteristics in Snap Bean (Phaseolus vulgaris) under Subtropical Environment. Japan Agricultural Research Quarterly, 2007, 41, 201-206.	0.4	3
330	ACE2 Expression in the Pancreas and Association With COVID-19 Infection. Pancreas, 2021, 50, e1-e2.	1.1	3
331	Variation of photon intensities in transmitted photon spectra of 60Co as a function of dimensions of a soil medium. Radiation Measurements, 2005, 39, 451-454.	1.4	2
332	An extremely wideband printed antenna with WLAN stop band using SRR. , 2014, , .		2
333	Constrained Dipole Oscillator Strength Distributions for CF <sub>4</sub> , CClF <sub>3</sub> , CCl <sub>2</sub> F <sub>2</sub> , CCl <sub>3</sub> F, CHF <sub>3</sub> , CH <sub>3</sub> F, CH <sub>3</sub> Cl, CH <sub>3</sub> Br, CH <sub>3</sub> I, C <sub>2</sub> F <sub>6</sub> , and CCl <sub>3</sub> CF <sub>3</sub> , Zeitschrift Fur Physikalische Chemie, 2016, 230, 1473-1486.	2.8	2
334	Design of quad-band microstrip-fed stubs-loaded frequency reconfigurable antenna for multiband operation. , 2017, , .		2
335	A Compact ACS-Fed Triple-Band Dual-Polarized Stubs-Loaded Frequency Reconfigurable Printed Antenna for WiMAX and WLAN Applications. , 2017, , .		2
336	Inner Loop Stability of Peak Current Controlled Cuk and SEPIC Converters. , 2018, , .		2
337	Derivation of Single-Stage Single-Phase Fourth Order Buck-boost Inverters. , 2018, , .		2
338	Effect of Mg2+ substitution on structural and magnetic properties of nano zinc ferrite. AIP Conference Proceedings, 2018, , .	0.4	2
339	Influence of La3+ ion doping on structural and magnetic properties of nickel ferrite nanoparticles prepared by sol-gel route. AIP Conference Proceedings, 2019, , .	0.4	2
340	Operating Modes based Review of Single-Stage Buck-Boost Inverters. , 2019, , .		2
341	Role of surfactant in optimization of 3D ZnO floret as photoanode for dye sensitized solar cell. Applied Nanoscience (Switzerland), 2020, 10, 1035-1044.	3.1	2
342	Responsive polymerâ€assisted 3D cryogel supports Huh7.5 as in vitro hepatitis C virus model and ectopic human hepatic tissue in athymic mice. Biotechnology and Bioengineering, 2021, 118, 1286-1304.	3.3	2

1

#	Article	IF	CITATIONS
343	Emergency Department Management of Mild Traumatic Brain Injury in New Delhi–A Single Institute Cohort Management Data. Indian Journal of Neurosurgery, 2022, 11, 123-127.	0.2	2
344	Effect of Add-On Therapy of Sodium-Glucose Cotransporter 2 Inhibitors and Dipeptidyl Peptidase 4 Inhibitors on Adipokines in Type 2 Diabetes Mellitus. Journal of Clinical Medicine Research, 2021, 13, 355-362.	1.2	2
345	Electronic and optical properties of boron-based hybrid monolayers. Nanotechnology, 2021, 32, 415203.	2.6	2
346	An RNAi-independent role of AP1-like stress response factor Pap1 in centromere and mating-type silencing in Schizosaccaromyces pombe. Journal of Biosciences, 2021, 46, 1.	1.1	2
347	Optimal vitamin D level ameliorates neurological outcome and quality of life after traumatic brain injury: a clinical perspective. International Journal of Neuroscience, 2023, 133, 417-425.	1.6	2
348	Targeted ablation of TRAF6 inhibits skeletal muscle wasting in mice. Journal of Experimental Medicine, 2011, 208, i2-i2.	8.5	2
349	Exploration of the B2O3-Bi2O3-MoO3 glass system based on its physical, optical, and gamma ray shielding capabilities. Optik, 2021, 248, 168177.	2.9	2
350	Loss of seed viability in onion (Allium cepa L.) in relation to degradation of lipids during storage. Journal of Applied and Natural Science, 2020, 12, 635-640.	0.4	2
351	Understanding the control of inclusion of SrO to the Li2O -K2O-B2O3-SrO glasses on the physical, structural, and gamma ray shielding performance. Journal of the Australian Ceramic Society, 2022, 58, 205-216.	1.9	2
352	Therapeutic plasma exchange in acute fatty liver of pregnancy: a case report and literature review. Pan African Medical Journal, 2021, 40, 220.	0.8	2
353	Hindi-English "mixing" in scientific discourse. World Englishes, 1985, 4, 355-358.	1.1	1
354	To the Editor. Journal of Orthopaedic Trauma, 2007, 21, 670.	1.4	1
355	Morphology dependent catalytic activity of TiO2 nanostructures towards photodegradation of Rose Bengal. AIP Conference Proceedings, 2015, , .	0.4	1
356	Frequency domain analysis and design of isolated bidirectional series resonant Dc-dc converter. , 2016, , .		1
357	Constrained dipole oscillator strength distributions, sum rules, and dispersion coefficients for Br 2 and BrCN. Chemical Physics Letters, 2017, 672, 31-33.	2.6	1
358	An extremely wideband/multiresonance monopole antenna with multiple notched stop bands. , 2017, , .		1
359	Design and analysis of a compact microstrip antenna using shorting pin for 5 GHz band. , 2017, , .		1

360 High aperture efficiency profiled horn at Ku-band. , 2017, , .

Ashok Kumar

#	Article	IF	CITATIONS
361	Behavior of lanthanum containing barium stannate nanoparticles synthesized by cetyltriammonium bromide assisted wet chemistry route. Materials Research Express, 2018, 5, 025030.	1.6	1
362	CCM-DCM Operation of a High Voltage Gain Boost-Flyback Derived Converter. , 2018, , .		1
363	Scope of Meta-Heuristics Optimizer for Automatic Generation Control of Realistic Power System. , 2019, , .		1
364	Redispersion of cryoaggregated gold nanoparticle by means of laser irradiation and effect on biological interactions. Nanotechnology, 2020, 31, 435601.	2.6	1
365	Angst, panic and stigma concomitant to COVID-19 deceased. Asian Journal of Psychiatry, 2021, 55, 102527.	2.0	1
366	Mechanical and Gamma-Ray Interaction Studies of PbO–MoO3–Li2O–B2O3 Glass System for Shielding Applications in The Low Energy Region: A Theoretical Approach. Applied Sciences (Switzerland), 2021, 11, 5538.	2.5	1
367	Effect of Add-On Therapy of Dapagliflozin and Empagliflozin on Adipokines in Type 2 Diabetes Mellitus. Journal of Endocrinology and Metabolism, 2021, 11, 83-90.	0.4	1
368	Nanocrystallite assembled La2CoNiO6 nanorods fabricated by facile solvothermal route for electrochemical performance. Journal of Nanoparticle Research, 2021, 23, 1.	1.9	1
369	LiKBPbX glasses: Physical, structural and gamma ray shielding competence. Optik, 2021, 247, 167835.	2.9	1
370	Structural, dielectric and magnetic properties of double perovskite-La2CoNiO6 ceramics synthesised by wet chemical route. International Journal of Nanotechnology, 2021, 18, 622.	0.2	1
371	Publication trend in the indian journal of orthopaedics: What is published and why?. Indian Journal of Orthopaedics, 2015, 49, 661.	1.1	1
372	Perceived effectiveness of infection control practices in Laundry of a tertiary healthcare centre. World Journal of Emergency Medicine, 2019, 10, 114.	1.0	1
373	Impact of replacement of B2O3 by TeO2 on the physical, optical and gamma ray shielding characteristics of Pb-free B2O3-TeO2-ZnO-Al2O3-Li2O-MgO glass system. Optik, 2021, 248, 168100.	2.9	1
374	Robot-assisted and conventional urology surgical procedures: comparison of average length of stay, economic status, operative time and patient's expenditure in a tertiary care hospital of North India. Journal of Robotic Surgery, 2022, , 1.	1.8	1
375	Giant congenital nevus. Indian Journal of Pediatrics, 1995, 62, 373-374.	0.8	0
376	Two Media Method: An Alternative Methodology for the Measurement of Attenuation Coefficients of Irregularly Shaped Samples. Nuclear Science and Engineering, 2008, 159, 338-345.	1.1	0
377	Analysis of Angelov model for 0.251̂¼m pHEMTs. Proceedings of SPIE, 2012, , .	0.8	0
378	Design, fabrication and measurement of sub 1 dB noise figure LNA. Proceedings of SPIE, 2012, , .	0.8	0

#	Article	IF	CITATIONS
379	Design of an extremely wideband quasi-self-complementary pentagonal antenna with WLAN stop band. , 2014, , .		Ο
380	Design and characterization of aperture coupled patch antenna for wearable applications. , 2017, , .		0
381	A triple-band dual-polarized compact square slot antenna with an offset CPW feeding and radiator. , 2017, , .		Ο
382	Two High Voltage Gain Non-isolated Dc-dc Converters with Ripple Free Input Current. , 2018, , .		0
383	Radiation interaction parameters of dosimetric importance for some commonly used compensators in IMRT using Monte Carlo simulation code. Journal of Radiological Protection, 2018, 38, 1321-1343.	1.1	Ο
384	A novel single myocapsular sleeve (SMS) repair technique to reduce dislocation in posterior approach to the hip: A clinico-radiographic study. Journal of Clinical Orthopaedics and Trauma, 2019, 10, S247-S251.	1.5	0
385	Scope of Artificial Intelligence for Interconnected Multi Area Power System: A Literature Review. , 2019, , .		0
386	The synthesis, structural, optical and electrical characterizations of double perovskite oxide Y2CuCoO5. AIP Conference Proceedings, 2020, , .	0.4	0
387	Asymmetric CPW-Fed Multistubs Loaded Compact Printed Multiband Antenna for Wireless Applications. Lecture Notes in Electrical Engineering, 2020, , 317-324.	0.4	0
388	Investigation of Substrate Integrated Waveguide (SIW) Filter Using Defected Ground Structure (DGS). Lecture Notes in Electrical Engineering, 2020, , 449-456.	0.4	0
389	Broadband Circularly Polarized CPW-Fed Inverted-L Grounded Strips and SRR Loaded Square Slot Antenna for Wi-Fi/WiMAX/5G Applications. Lecture Notes in Electrical Engineering, 2020, , 591-596.	0.4	0
390	Alkaline Earth Stannate Nanomaterials as an Electron Transport Layer in Dye-Sensitized Solar Cells. , 2021, , 1-22.		0
391	X- ray absorption parameters studies of P2O5- SnCl2-SnO bioactive glass system. Journal of X-Ray Science and Technology, 2021, 29, 373-382.	1.0	Ο
392	Optical and gamma ray shielding properties BaO doped K2O-TiO2-P2O5 glasses. Optik, 2021, 247, 167893.	2.9	0
393	B2O3-TeO2-K2O-Li2O glasses: Optical and gamma ray shielding characterization. Optik, 2021, 247, 167847.	2.9	Ο
394	EVALUATION OF DIAGNOSTIC PARAMETERS TO DETECT INDUCTION OF ACNE, ACUTE DERMAL IRRITATION AND CORROSION POTENTIAL OF A POLYHERBAL FORMULATION. International Journal of Research in Ayurveda and Pharmacy, 2017, 8, 87-90.	0.1	0
395	Effect of Annealing on Structural Properties of Fe3O4 Ferrite Nanoparticles. Advanced Science Letters, 2018, 24, 5748-5751.	0.2	0
396	Management of hunger strike: A medical, ethical and legal conundrum. Medico-Legal Journal, 2020, 88, 215-219.	0.5	0

#	Article	IF	CITATIONS
397	Comparison of Ultrasonography and X-Rays for the Diagnosis of Synovitis and Bony Erosions in Small Joints of Hands in Early Rheumatoid Arthritis: a Prospective Study. Mædica, 2021, 16, 22-28.	0.1	0
398	Fire incidents in Bed-head panels: Causes and recommendations for prevention. Journal of Family Medicine and Primary Care, 2022, 11, 360.	0.9	0